Design of PID, IMC and IMC based PID Controller for Hydro Turbine Power System of Non-minimum Phase Dynamics

Supriya Y. Bhuran [1*], Sharad P. Jadhav [2]
[1,2] Department of Instrumentation Engineering, Ramrao Adik Institute of Technology, Navi Mumbai, India
Email: [1] supriya.bhuran@rait.ac.in, [2] sharad.jadhav@rait.ac.in
*Corresponding Author

Abstract—**The primary objective of this paper is to design and assess the performance of conventional Proportional Integral Derivative (PID), Internal Model Controller (IMC), and IMC-based PID controllers tailored for Hydro Turbine Power Systems (HTPS) exhibiting Non-Minimum Phase (NMP) dynamics. The focus is on overcoming the limitations of existing approaches in handling such complex system dynamics. Existing literature underscores the difficulty of crafting controllers for such systems. The current study represents a sincere endeavour to design and evaluate the performance of conventional Proportional Integral and Derivative (PID), Internal Model Controller (IMC), and IMC-based PID controllers tailored for HTPS characterized by NMP behaviour. The design case study and simulations were conducted using MATLAB and Simulink. The closed-loop responses of HTPS with PID, IMC, and IMC-PID are presented, and the controller performances are scrutinized in both time and frequency domains. To validate the effectiveness of the controllers, performance indices such as Integrated Squared Error (ISE), Integrated Absolute Error (IAE), Integrated Time-weighted Absolute Error (ITAE), Integrated Time Squared Error (ITSE) are calculated, as well as control efforts are calculated using 2-norm and infinity-norms. These performance indices and control effort norms offer a comprehensive evaluation of the controllers' performance in terms of minimizing error, handling system dynamics, and optimizing control effort across different time scales. Analysing these metrics aids in selecting and refining controllers for optimal performance in HTPS with NMP behaviour. Our findings illustrate that IMC-based PID controllers exhibit superior performance compared to conventional PID controllers in effectively handling the Non-Minimum Phase (NMP) dynamics of Hydro Turbine Power Systems (HTPS). This superiority is substantiated by enhanced performance indices, including reductions in ISE, IAE, ITSE, and ITAE.**

***Keywords*—*Non-Minimum Phase; Hydro Turbine Power System; PID; IMC; IMC based PID; Control System; System Dynamics*.**

I. Introduction

This paper tackles the formidable challenge of designing Load Frequency Controllers (LFC) specifically tailored for Hydro Turbine Power Systems (HTPS) characterized by Non-Minimum Phase (NMP) dynamics. Preserving stability in power systems is paramount, especially in response to abrupt alterations in load or generation. This diligence is essential to avert blackouts and uphold the dependable provision of electricity. Load Frequency Control (LFC) emerges as a pivotal function within power systems, tasked with preserving the equilibrium between the generated electric energy and the demand from loads. The effective management of this balance is crucial for sustaining the stability and reliability of the overall power grid [1]- [4]. In essence, LFC ensures that the electricity generated aligns with the varying demands, safeguarding against potential disruptions and contributing to the seamless functioning of our interconnected electrical systems [5]- [7]. The Load Frequency Controller (LFC) plays a pivotal role in aligning power supply with demand, thereby preserving the stability of the grid. Its effectiveness extends to minimizing losses in the power system by mitigating the necessity for costly additional generation and transmission capacity [8]- [10]. This reduction in infrastructure needs contributes to cost savings in both construction and maintenance. Furthermore, LFC enhances the operational efficiency of the power system by enabling generators to operate at their optimal output levels. This not only reduces fuel consumption but also leads to a decrease in emissions, aligning with sustainable and environmentally conscious practices.

This paper focuses on the Hydro Turbine Power System (HTPS), encompassing components such as the governor model, turbine model, generator & load model, and droop characteristics. The literature survey conducted delves into various power system models and commonly employed control strategies in traditional power systems, incorporating soft computing techniques. Different turbine models, including thermal, gas, hydro, reheat steam, non-reheat steam, and combinations of these, are discussed in existing literature [11]. These turbine models serve as the basis for defining the types of power systems. Notably, among the available models, this paper specifically addresses the hydro turbine model with Non-Minimum Phase (NMP) dynamics.

In the realm of control systems theory, non-minimum phase dynamics pertain to the presence of additional zeros in the Right Half of the S-plane (RHS) [12]- [13]. This characteristic introduces complexity to stability analysis and controller design, often leading to potentially unstable behaviour. Hydro Turbine Power Systems (HTPS) featuring Non-Minimum Phase (NMP) dynamics present specific challenges in control; issues include unstable behaviour, delayed responses, and difficulties in achieving precise control [14]- [17]. Consequently, these challenges contribute to slower system performance, reduced disturbance rejection capabilities, instability, oscillations, the need for delay compensation, and limited effectiveness in rejecting disturbances. Additionally, the design of controllers for systems with NMP dynamics must consider modeling uncertainties and variations in system parameters, highlighting the intricacies involved in achieving stable and efficient control in such systems.

To address such control challenge traditional controllers like PID, Smith Predictor, lead-lag compensators, and feedforward control have been used for system under investigation. In the paper [18] Dual loop – internal model control (DL-IMC) scheme is proposed for hydrothermal power plant for disturbance rejection and minimization of oscillations. The tread-off between the closed loop performance and robustness of the IMC based PID controller for NMP integrating processes with time delays are presented in [15]. IMC based controllers for good set point tracking and disturbance rejection for specific NMP systems are presented in [19]. The performances of above discussed controllers are having some limitations. From the literature it is observed that there is need of designing an effective and efficient controller for HTPS with NMP behaviour [62]- [64].

This paper presents design and investigate the performance of conventional Proportional Integral and Derivative (PID) [20]- [27], Internal Model Controller (IMC) [28]- [32]and IMC based PID controllers [44]- [52]for HTPS of NMP behaviour. From the simulation results it is concluded that the IMC based control strategy handles NMP dynamics of HTPS more effectively as compared to conventional PID controllers. Rest of the paper is organized as, in section 2 non-minimum phase hydro turbine power system's mathematical model is presented. In section 3 & 4 designing of PID controller, IMC controller and IMC based PID controller is explained. Section 5 covers the performance analysis in terms of time domain, frequency domain & different error calculations and then results and discussion covered in 6th section; Conclusion is in section 7.

II. Modelling of Hydro Turbine Power System (HTPS)

The hydro turbine is used to generate electricity in hydroelectric power generation plants where energy is transferred from moving water to rotating shaft. The block diagram of the single area hydro turbine power system which exhibits non-minimum phase dynamics is shown in Fig. 1; which consist of governor Fig. 2, hydro turbine Fig. 3 and generator with load Fig. 4 and primary controller i.e., droop characteristics [66]- [72].

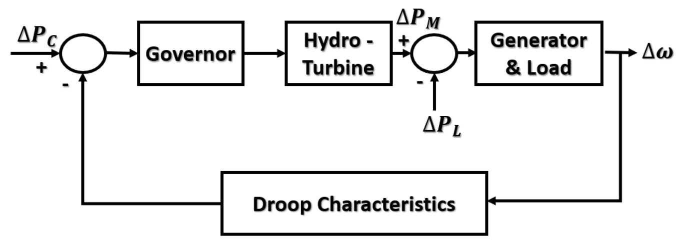

Fig. 1. Hydro Turbine Power system (HTPS).

A. The Governor

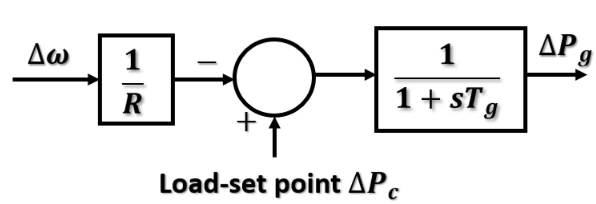

Fig. 2. Typical Governor block diagram.

$$\frac{\Delta P_g}{\Delta \omega} = \frac{-(\frac{1}{R})}{1+T_g s} \tag{1}$$

B. Hydro Turbine Model

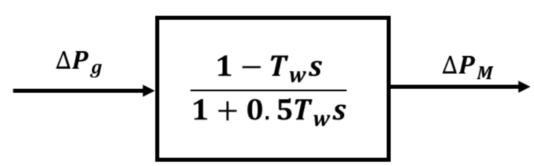

Fig. 3. Hydro Turbine block diagram.

$$\frac{\Delta P_M}{\Delta P_g} = \frac{1-T_w s}{1+0.5T_w s} \tag{2}$$

C. Hydro Turbine Model

$$\frac{\Delta P_M - \Delta P_L}{\Delta \omega} = \frac{K_p}{1+T_p s} \tag{3}$$

The transfer function of the block diagram as shown in Fig. 1, obtained using a block reduction method and can be written as given in (4).

$$\frac{\Delta \omega}{\Delta P_c} = \frac{(1-T_w s)(K_p)}{(1+T_g s)(1+0.5T_w s)(1+T_p s)+\frac{1}{R}} \tag{4}$$

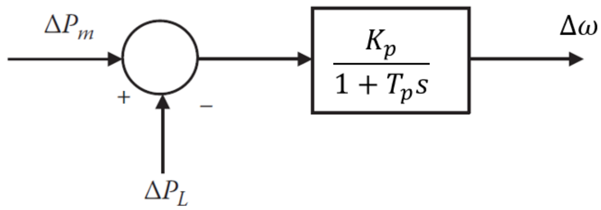

Fig. 4. Generator and Load model block diagram.

The different variables used in modelling of NMP HTPS are listed in Table I. The values of above listed parameters used to identify the transfer function are Kp = 1, Tp = 6, Tw = 4, Tg = 0.2 and R = 0.05 [54], [62].

TABLE I. NOMENCLATURE

ΔP_L	External load change (p.u.MW)
ΔP_g	The change in steam valve position
ΔP_m	The change in turbine mechanical power output
$\Delta\omega$	Speed deviation (input to governor) due to load change (Hz)
ΔP_c	Load set-point
T_g	Time constant of the governor (s)
R	The speed droop regulation constant.
T_w	The Hydro-turbine time constant (s)
K_p	Gain of electric system
T_p	Time constant electric system (s)

After utilising all given parameter values and substituting in equation (4) the final transfer function is,

$$G_p(s) = \frac{\Delta\omega}{\Delta P_c} = \frac{(1-4s)}{2.4s^3 + 13.6s^2 + 8.2s + 21}. \quad (5)$$

After examining the equation (4) & equation (5), it is very much clear that system's zero lies in right-half of the complex plane and thus the above-mentioned system is non-minimum phase system [63]- [65]. The root locus of system is shown in Fig. 5 which clearly shows that due to zero at right half of complex plane the system becomes unstable. The critical gain of the system is approximately 1.14 when it travels from stability to instability whereas the damping ratio is negative.

III. CONTROLLER DESIGN FOR HTPS WITH NMP DYNAMICS

A. Conventional PID Controller

The PID controller is connected as secondary controller to the non-minimum phase single area power system as shown in Fig. 6 [11].

The mathematically PID controller is expressed in (6) as,

$$G_c(s) = K_p(1 + \frac{1}{T_i}s + T_d s), \quad (6)$$

where Kp is proportional gain, Ti is integral time constant and Td is derivative time constant [58]- [59].

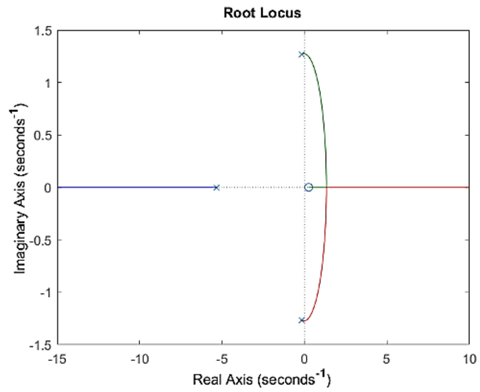

Fig. 5. Root Locus plot of NPS HTPS.

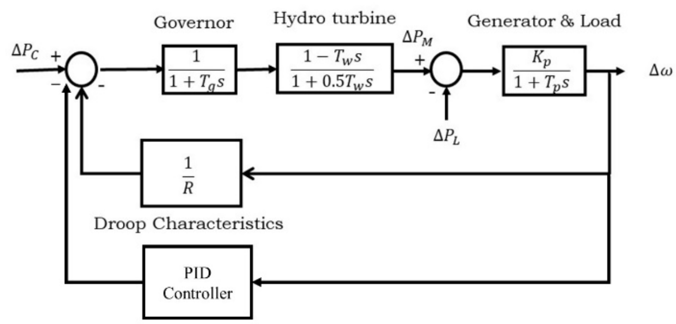

Fig. 6. PID Controller for NMP HTPS

The final transfer function of system with secondary PID controller can be obtained using (7) as,

$$\frac{\Delta\omega}{\Delta P_c} = \frac{(1-T_w s)(K_p)}{(1+T_g s)(1+0.5T_w s)(1+T_p s) + (\frac{1}{R} + G_c(s))}. \quad (7)$$

The transfer function of PID is,

$$C_{PID} = \frac{1.019e^{-8}s^2 + 1.287e^{-5}s + 0.00406}{0.00317s} \quad (8)$$

B. Proposed Internal Model Control (IMC) method

The IMC was introduced by Garcia and Morari. IMC is a control strategy that explicitly incorporates an internal model of the system dynamics, allowing it to handle non-minimum phase behaviour more effectively compared to traditional controllers. The standard feedback structure uses the process model in an implicit fashion, that is, PID tuning parameters are "tweaked" on a transfer function model, but it is not always clear how the process model effects the tuning decision [32], [33], [34]. By including an internal model that represents the system's dynamics, IMC effectively accounts for the unstable poles and zeros in the design process. The IMC controller can effectively handle the time delays and improve control performance, leading to faster response times and better accuracy [35]- [40]. The internal model serves as a representation of the system's dynamics, allowing the controller to adapt and compensate for uncertainties effectively [41]- [43]. This robustness to model uncertainty is particularly beneficial in non-minimum phase systems where variations and uncertainties can have a significant impact on control performance [55]- [56]. The basic structure of IMC is shown in Fig. 7. From the Fig. 7; we can say that the original plant model G(s) is compared with its plant developed model $\widetilde{G}(s)$which creates the feedback signal $\widetilde{D}(s)$. The feedback signal can be mathematically expressed as in (9).

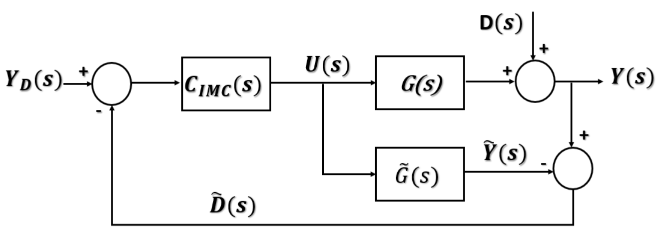

Fig. 7. The basic structure of IMC based controller.

$$\widetilde{D}(s) = (G(s) - \widetilde{G}(s))U(s) + D(s), \tag{9}$$

where, $D(s)$ is the Laplace transform of the external disturbance $d(t)$. In some conditions if external disturbance is absent then $D(s) = 0$ which provides the actual difference between the plant model $G(s)$ and developed model $\widetilde{G}(s)$ to feedback signal $\widetilde{D}(s)$. Therefore the $\widetilde{D}(s)$ is useful to improve the control signal if it is subtracted from $Y_D(s)$.

Thus, the control signal $U(s)$ can be obtained from block diagram and represented in (10),

$$U(s) = C_{IMC}(s)(Y_D(s) - \widehat{D}(s)). \tag{10}$$

Substituting (9) in (10) gives,

$$U(s) = C_{IMC}(s)(Y_D(s) - (G(s) - \widetilde{G}(s))U(s) + D(s)). \tag{11}$$

$$U(s) = C_{IMC}(s)Y_D(s) - C_{IMC}(s)G(s)U(s)$$
$$+C_{IMC}(s)\widetilde{G}(s)U(s) - C_{IMC}(s)D(s), \tag{12}$$

and final representation is shown in (13) as,

$$\therefore U(s) = \frac{C_{IMC}(s)(Y_D(s) - D(s))}{1 + C_{IMC}(s)(G(s) - \widetilde{G}(s))}. \tag{13}$$

IMC controller designing is done in step-wise procedure as,

Step 1: Derive positive part of plant model which consist of all delays in system and any positive zero;

Step 2: Derive negative part of plant model which consist of negative zeros and remaining components of plant;

Step 3: Choose appropriate low pass filter which ensure the properness and speed of the IMC controller [57].

The plant model is separated in positive and negative parts.

$$\widetilde{G}(s) = \widetilde{G}_+(s)\widetilde{G}_-(s), \tag{14}$$

the factor $\widetilde{G}_+(s)$ contains all time delays and positive zeros and, the factor $\widetilde{G}_-(s)$ has no delays and all of its zeros are negative. IMC controller is given as,

$$C_{IMC}(s) = (\frac{1}{\widetilde{G}_-(s)})LPF(s). \tag{15}$$

And $LPF(s) = \frac{1}{(1+T_f s)^\eta}$ is low pass filter selected such a way that IMC controller is proper. Thus, η is selected to achieve properness of IMC controller, T_f is speed response adjustable parameter. Also, the closed loop system output Y(s) is determined as $Y(s) = G(s)U(s) + D(s)$; which is derived as,

$$Y(s) = G(s)\left(\frac{C_{IMC}(s)(Y_D(s) - D(s))}{1 + C_{IMC}(s)\left(G(s) - \widetilde{G}(s)\right)}\right) + D(s), \tag{16}$$

i.e. $Y(s) = \left(\frac{G(s)\widetilde{G}_-^{-1}(s)F(s)}{1+\widetilde{G}_-^{-1}(s)F(s)\left(G(s)-\widetilde{G}(s)\right)}\right)Y_D(s)$

$$+\left(\frac{1 - \widetilde{G}(s)\widetilde{G}_-^{-1}(s)F(s)}{1 + \widetilde{G}_-^{-1}(s)F(s)\left(G(s) - \widetilde{G}(s)\right)}\right)D(s), \tag{17}$$

where the sensitivity function,

$$S_f(s) = \left(\frac{1-\widetilde{G}(s)\widetilde{G}_-^{-1}(s)F(s)}{1+\widetilde{G}_-^{-1}(s)F(s)\left(G(s)-\widetilde{G}(s)\right)}\right),$$

and complementary sensitivity function,

$$CS_f(s) = \left(\frac{G(s)\widetilde{G}_-^{-1}(s)F(s)}{1+\widetilde{G}_-^{-1}(s)F(s)\left(G(s)-\widetilde{G}(s)\right)}\right).$$

If the developed plant model is very accurate to original plant model, then; mismatch is zero then sensitivity $S_f(s) = 0$ and complementary sensitivity $CS_f(s) = 1$. In such condition the input tracking will be accurate and external disturbance rejection can be achieved successfully. Fig. 8 illustrates the connection of the Internal Model Control (IMC) controller in a closed-loop system with the plant model.

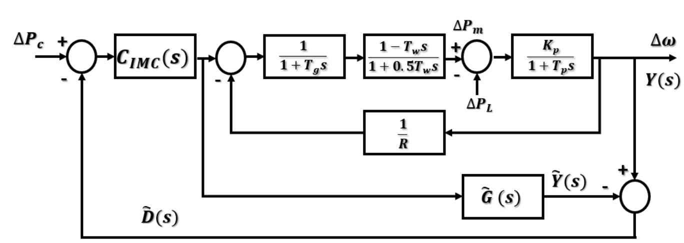

Fig. 8. Closed loop system with IMC controller

To guarantee the properness of the IMC controller for the given system, a value of $\eta = 3$ is selected. The parameter T_f is chosen as 2.0 to fine-tune the speed response. The resulting transfer function of the IMC controller is provided in equation (18).

$$C_{IMC} = \frac{2.4s^3 + 13.6s^2 + 8.2s + 21}{8s^3 + 12s^2 + 6s + 1}. \tag{18}$$

C. Internal Model Control based Proportional Integral Derivative (IMC based PID) Controller

The classical controller is connected in a cascaded configuration with the plant, forming a closed-loop system, as illustrated in Fig. 9.

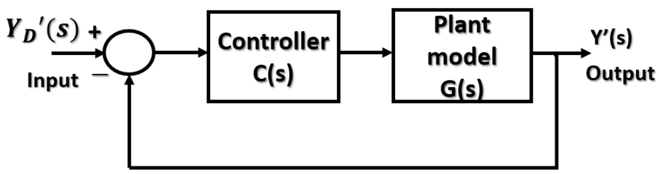

Fig. 9. Classical controller in closed loop system

In the process of designing the Internal Model Control (IMC) based PID controller, Fig 7 and 9 were thoroughly examined. The relationship between the IMC and IMC-based PID controllers was investigated by analysing the general closed-loop transfer functions without the presence of external disturbances. Consequently, the transfer function equation (16) of the IMC-based controller without disturbance is derived as,

$$\frac{Y(s)}{Y_D(s)} = \frac{G(s)C_{IMC}(s)}{1 + C_{IMC}(s)(G(s) - \widetilde{G}(s))}. \tag{19}$$

The transfer function of closed loop system with classical controller and without disturbance is,

$$\frac{Y\prime(s)}{Y_D\prime(s)} = \frac{G(s)C(s)}{1 + G(s)C(s)}. \tag{20}$$

After analysing equation (19) and equation (20), IMC based PID controller is given in equation (22),

$$\frac{G(s)C_{IMC}(s)}{1 + C_{IMC}\left(G(s) - \widetilde{G}_-(s)\right)} = \frac{G(s)C(s)}{1 + G(s)C(s)}. \tag{21}$$

$$\therefore\ C(s) = \frac{C_{IMC}(s)}{1 - C_{IMC}(s)\widetilde{G}(s)}\ . \tag{22}$$

Now equation (22) with equation (14) and equation (15) becomes

$$C(s) = \frac{(\frac{1}{\widetilde{G}_-(s)})F(s)}{1 - F(s)\widetilde{G}_+(s)}$$

i.e.,

$$C(s) = \frac{\widetilde{G}_-^{-1}(s)}{F^{-1} - \widetilde{G}_+(s)}. \tag{23}$$

The plant transfer function as shown in equation (5), can be reduced to second order system by using two dominant poles. The characteristics equation of the system is ($2.4s^3 + 13.6s^2 + 8.2s + 21$). The roots of the system are ($-5.3337,\ -0.1665 \pm 1.2700i$). The real root can be neglected as the real part of the complex conjugate roots is less than one-fifth of the real root [5]. Thus, the reduced order i. e. second order model of plant is,

$$\widetilde{G_r}(s) = \frac{k\ (1 - 4s)}{s^2 + 0.333s + 1.641}, \tag{24}$$

where k is chosen as $k = 1.641/(1 + 1/R) = 0.078$; such that DC gains of original plant and reduced order plant are equivalent. To verify the alignment between the original plant and the reduced-order plant model, the step responses of both are plotted, as illustrated in Fig. 10. The responses of both transfer functions exhibit a close match, indicating a high degree of similarity. Consequently, it can be inferred that the dynamics of the two systems are consistent.

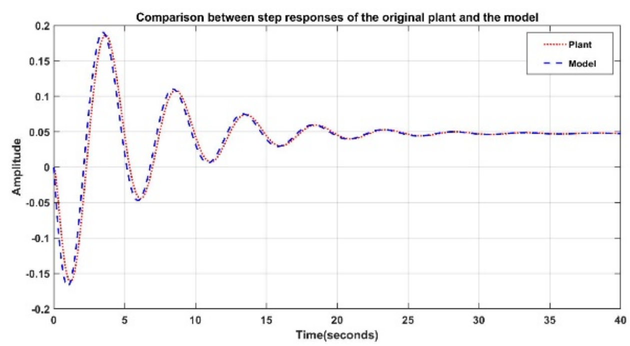

Fig. 10. Step response of original vs reduced ordered model.

Now, to design IMC based PID controller, the plant model is separated in positive and negative parts.

$$\widetilde{G}_r(s) = \widetilde{G}_{r+}(s)\widetilde{G}_{r-}(s) \tag{25}$$

$\therefore \widetilde{G_{r+}}(s) = 0.078\,(1 - 4s)$ and

$$\widetilde{G}_{r-}(s) = \frac{1}{s^2 + 0.333s + 1.641}. \tag{26}$$

For IMC based PID controller equation (22) can be re-written using equation (24) and LPF i.e., $\frac{1}{(1+T_f s)^r}$ as with $T_f = 1$ & $r = 2$.

$$C_{IMC\_PID} = \frac{s^2 + 0.333s + 1.641}{(1 + T_f s)^r - 0.078\ (1 - 4s)}, \tag{27}$$

$$C_{IMC\_PID} = \frac{s^2 + 0.333s + 1.641}{4s^2 + 6.882s - 0.0105}. \tag{28}$$

IMC based PID controller is cascaded with original plant model with unity feedback is as shown in Fig. 11. The IMC-based PID controller is connected in a cascaded configuration with the original plant model, and the entire system operates under unity feedback, as depicted in Fig 11.

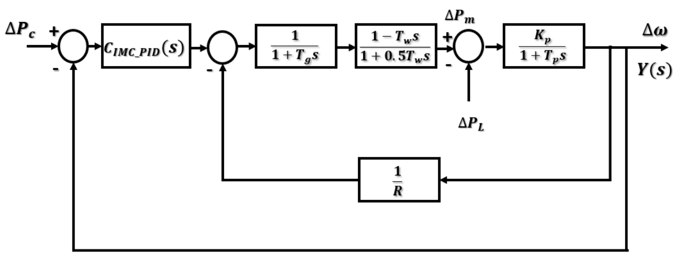

Fig. 11. Closed loop system with IMC based PID controller

IV. Closed loop Analysis of PID, IMC and IMC based PID controllers

To conduct a comprehensive performance analysis of PID, IMC-based controller, and IMC-based PID controller, simulations were carried out using the MATLAB software within the online MATLAB environment. The simulation and programming for the Non-Minimum Phase hydro turbine power system (NMP HTPS) were implemented using MATLAB's live script. The tuning of the PID controller for the plant was accomplished using the 'pidtune' function within the live script.

The primary objective of this simulation-based study was to assess and compare the performance of the conventional PID controller with the model-based Internal Model Controller (IMC) and the IMC-based PID controller. The initial phase involved the design and simulation of the PID controller using MATLAB programming within a live script. Similarly, scripts were written for the design of the IMC and IMC-based PID controllers.

Utilizing MATLAB/Simulink programming, the investigation encompassed both step response and the impact of a 20% load change as an external disturbance on the NMP HTPS. The controllers were applied in the secondary control loop, as illustrated in Fig. 6, 8 and 10 for PID, IMC, and IMC-based PID controllers, respectively. Time domain parameters such as rise time, settling time, overshoot, and undershoot were analysed for both controllers using the 'stepinfo' syntax. Additionally, frequency response analysis parameters were calculated using the bode plot.

Fig. 12 visually represents the step response of the system without a controller, with a PID controller, with an IMC-based controller, and with an IMC-based PID controller. The system with the PID controller exhibits oscillations in transient response and takes around 47 seconds to stabilize the frequency deviation i.e. $\Delta\omega$, reflecting the challenge in tuning a PID controller for the RHS zero of the NMP HTPS.

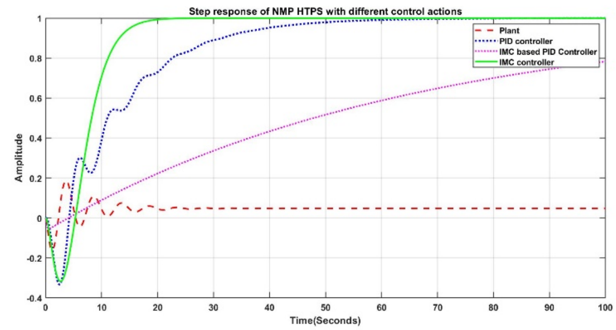

Fig. 12. Step response of NMP HTPS with different control actions

Tuning a PID controller to strike a suitable balance between various control objectives is intricate, leading to challenges in achieving optimal performance in all aspects simultaneously. The IMC-based PID controller requires more time to rise and reach the set point, as highlighted in Table III. Fig. 13 depicts the system response for various designed controllers in the presence of a 20% load change.

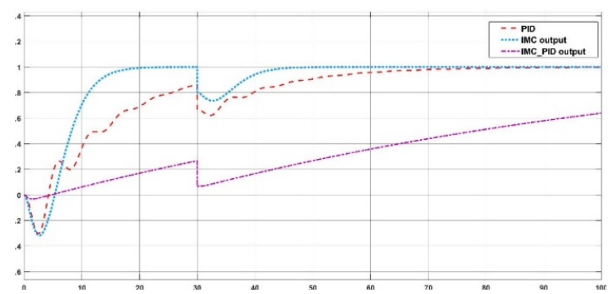

Fig. 13. Response of NMP HTPS with 20% load change

A. Time Domain Analysis

The comparison of PID, IMC, and IMC-based PID controllers in the time domain is presented in Table II. Notably, the IMC controller exhibits improvements in both rise time and settling time compared to the PID and IMC-based PID controllers. All controllers successfully mitigate overshoot.

Introducing a 20% load change as an external disturbance at t=30 sec, the time domain parameters are re-evaluated and documented in Table III. The IMC controller, featuring an internal model representing the system's dynamics, effectively addresses the challenges posed by an unstable zero during the design phase. This incorporation leads to enhanced stability margins and a reduced likelihood of system instability or oscillations. The non-minimum phase behavior of the NMP HTPS results in a delayed response that impacts control performance. The internal model within the IMC controller captures the intricacies of the system's dynamics, including the non-minimum phase behavior. This capability enables the controller to anticipate and counteract disturbances, resulting in superior disturbance

TABLE II. TIME DOMAIN ANALYSIS

Transient Response	Open Loop	PID Controller	IMC Based PID Controller	IMC Controller
Rise Time (s)	0.1729	26.9175	140.1897	7.3331
Settling Time (s)	23.9371	47.0059	252.5376	16.7570
Overshoot	291.7782	0	0	0
Undershoot	340.7513	33.2084	1.8067	31.7474

rejection performance compared to traditional controllers. The internal model serves as a representative depiction of the system's dynamics, empowering the controller to adapt and compensate for uncertainties. This robustness to model uncertainty proves particularly advantageous in non-minimum phase systems, where variations and uncertainties can significantly influence control performance. The study underscores the efficacy of the IMC controller in enhancing stability, responsiveness, and disturbance rejection in the challenging context of NMP HTPS.

TABLE III. TIME DOMAIN ANALYSIS WITH 20% LOAD CHANGE

Transient Response	PID Controller	IMC based PID Controller	IMC Controller
Rise Time (s)	19.799	136.558	7.380
Settling Time (s)	57.481	269.696	14.726
Overshoot	0	0	0
Undershoot	4.622	0.02047	6.695

B. Frequency Analysis Using Bode Plots

The frequency response of a system provides insights into its steady-state behaviour when subjected to sinusoidal inputs of varying frequencies. Parameters such as phase margin and gain margin offer crucial information regarding the system's stability across different frequencies. The specific parameters extracted from Fig. 14 are documented in Table IV.

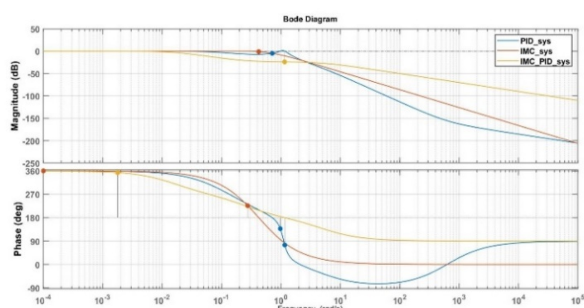

Fig. 14. Bode plot of PID, IMC based PID & IMC Controller

Upon scrutinizing the designed controllers, a notable observation emerges: IMC-based controllers exhibit greater stability compared to the conventional PID controller. Notably, the IMC-based PID controller demonstrates enhanced stability and resilience to disturbances. This improvement is evident in the increased gain and phase margins when compared to both the PID controller and the standard IMC controller.

TABLE IV. FREQUENCY DOMAIN ANALYSIS

Frequency Response	PID Controller	IMC based PID Controller	IMC Controller
Gain Margin (db)	4.8563	24.0226	1.1598
Phase Margin	-42.6284	173.0786	45.8094
Gain crossover Frequency	0.9778	0.0018	0.2751
Phase crossover Frequency	0.7129	1.1524	0.4226

However, when we juxtapose the findings from frequency domain analysis with those from time domain analysis, a nuanced insight emerges. In the present context, the IMC controller stands out as more suitable than the IMC-based PID controller. This suggests that, despite the enhanced stability of the IMC-based PID controller in the frequency domain, the IMC controller offers superior performance considering the overall system dynamics and requirements.

C. Performance Indices

All errors, namely Integral Square Error (ISE), Integral Absolute Error (IAE), Integral Time Square Error (ITSE), and Integral Time Absolute Error (ITAE), have been computed and organized in Table V. Analysis of these values reveals that superior system response speed and accuracy are attained when employing the IMC controller. Specifically, the IMC controller exhibits lower values for integral square error, integral absolute error, integral time square error, and integral time absolute error in comparison to both PID and IMC-based PID controllers. This suggests that the IMC controller outperforms the others in achieving a more precise and efficient system response.

TABLE V. PERFORMANCE INDICES

Error Calculations	PID Controller	IMC based PID Controller	IMC Controller
ISE	11.3005	8.5953	4.125
IAE	16.3743	9.3558	6
ITSE	8113.1	1432.7	462.5
ITAE	195.9649	93.0478	23.9992

D. Control Effort

The control effort refers to the quantity of energy or power required by the controller to carry out its designated function.

- 2-norm of Control Effort:
  Represents the Euclidean norm of the control effort, providing a measure of the overall magnitude of the

control input.

$$\| u(t) \|_2 = \sqrt{\int_0^T |u(t)|^2 \, dt} \quad (29)$$

- Infinity-norm of Control Effort:
  Captures the maximum magnitude of the control effort throughout the specified time period.

$$\| u(t) \|_\infty = max_t u(t) \quad (30)$$

In this study, the calculation of 2-norm and infinity-norm values has been calculated and documented in Table VI. This allows for the examination of control efforts associated with each controller. These performance indices and control effort norms offer a comprehensive evaluation of the controllers' performance in terms of minimizing error, handling system dynamics, and optimizing control effort across different time scales.

TABLE VI. 2-NORM AND ∞ NORM VALUES

Norm Calculations	PID Controller	IMC Based PID Controller	IMC Controller
2-Norm	0.4941	0.6996	0.3062
∞-Norm	1.1383	1.0964	1.0

Analysing these metrics aids in selecting and refining controllers for optimal performance in HTPS with NMP behaviour. Remarkably, the IMC controller demonstrates lower control efforts compared to the other two controllers. This observation suggests that the IMC controller excels in delivering efficient performance with reduced energy requirements, highlighting its effectiveness in achieving superior control outcomes.

V. RESULTS AND DISCUSSION

The MATLAB simulation provides clear evidence that both Internal Model Control (IMC) and Proportional-Integral-Derivative (PID) controllers demonstrate effectiveness in managing non-minimum phase systems. However, it becomes apparent that IMC controllers are more adept in handling these systems due to their capability to consider the impacts of zeros in the right half-plane. Moreover, IMC controllers offer built-in tuning rules that streamline the design process. In comparison, even with 20% load change condition showing that the IMC-based controller stands out by delivering superior accuracy and speed in the system's response. This distinction underscores the advantage of using IMC controllers, emphasizing their suitability for non-minimum phase systems. Overall, the findings highlight the practical advantages and efficiency of IMC controllers in such scenarios, providing valuable insights for control system design.

VI. CONCLUSION

This paper presents a mathematical model for Hydro Turbine Power System (HTPS) exhibiting Non-Minimum Phase (NMP) behaviour. The study addresses the complex task of Load Frequency Control (LFC) in HTPS by devising controllers, including Proportional-Integral-Derivative (PID), Internal Model Control (IMC), and a combined IMC-PID approach. The performance of these controllers is thoroughly analysed in both the time and frequency domains through simulation.The simulation results reveal that the IMC-based control strategy, incorporating an internal model of system dynamics, outperforms conventional PID controllers in effectively handling the NMP dynamics of HTPS. To validate the controllers' efficacy, a comparative analysis is conducted based on performance indices criteria and control efforts norms. The study emphasizes that traditional tuning methods are not directly applicable to meet LFC requirements in HTPS with NMP characteristics.

The IMC design is highlighted for its ability to offer flexibility in adjusting internal model parameters, enabling optimization of controller performance. Furthermore, the paper suggests the potential application of soft computing optimization approaches to achieve desired response characteristics in the investigated system. This implies a promising avenue for refining control strategies in scenarios with non-standard dynamics. In summary, the research contributes a comprehensive understanding of LFC in HTPS with NMP behavior, showcasing the superiority of IMC-based controllers over PID counterparts. The findings underscore the need for specialized tuning methods and highlight the adaptability and optimization capabilities of IMC design.

The soft computing optimization introduces an exciting prospect for future advancements in achieving desired system responses, like developing hybrid controllers [61] or using artificial intelligence or optimization techniques [60] for further optimization of control strategies in NMP systems. Additionally, the power system encompasses various turbines, including thermal and nuclear types, and features single area, double area, and multi-area systems [73]- [80]. The incorporation of these elements is a potential avenue for future work.

REFERENCES

[1] S. Chang and S. Qi, "Design and analysis of a load frequency control system based on improved artificial intelligence control algorithm," *Alexandria Engineering Journal*, vol. 61, no. 12, pp. 11779–11786, 2022, doi: 10.1016/j.aej.2022.05.026.

[2] N. Jalali, H. Razmi, and H. D. Mojarrad, "Optimized fuzzy self-tuning PID controller design based on tribe-de optimization algorithm and rule weight adjustment method for load frequency control of interconnected multi-area power systems," *Applied Soft Computing*, vol. 93, 2020, doi: 10.1016/j.asoc.2020.106424.

[3] H. H. Alhelou and M. E. Golshan, "Chapter 11-Decision-making-based optimal generation-side secondary-reserve scheduling and optimal LFC in deregulated interconnected power system," *Decision Making Applications in Modern Power Systems*, pp. 269–299, 2020, doi: 10.1016/B978-0-12-816445-7.00011-6.

[4] M. A. R. Shafei, D. K. Ibrahim, and M. Bahaa, "Application of PSO tuned fuzzy logic controller for LFC of two-area power system with redox flow battery and PV solar park," *Ain Shams Engineering Journal*, vol. 13, no. 15, 2022, doi: 10.1016/j.asej.2022.101710.

[5] I. A. Khan, H. Mokhlis, N. N. Mansor, H. A. Illias, L. J. Awalin, and L. Wang, "New trends and future directions in load frequency control and flexible power system: A comprehensive review," *Alexandria Engineering Journal*, vol. 71, pp. 263–308, 2023, doi: 10.1016/j.aej.2023.03.040.

[6] E. M. Ahmed, E. A. Mohamed, A. Selim, M. Aly, A. Alsadi, W. Alhosaini, H. Alnuman, and H. A. Ramadan, "Improving load frequency control performance in interconnected power systems with a new optimal high degree of freedom cascaded FOTPID-TIDF controller," *Ain Shams Engineering Journal*, vol. 14, no. 10, 2023, doi: 10.1016/j.asej.2023.102207.

[7] B. Dhanasekaran, J. Kaliannan, A. Baskaran, N. Dey, and J. M. R. S. Tavares, "Load frequency control assessment of a PSO-PID controller for a standalone multi-source power system," *Technologies*, vol. 11, no. 1, 2023, doi: 10.3390/technologies11010022.

[8] R. E. Sehiemy, A. Shaheen, A. Ginidi, and S. F. A. Gahtani, "Proportional-integral-derivative controller based-artificial rabbits' algorithm for load frequency control in multi-area power systems," *Fractal and Fractional*, vol. 7, no. 1, 2023, doi: 10.3390/fractalfract7010097.

[9] B. Khokhar and K. P. S. Parmar, "Utilizing diverse mix of energy storage for LFC performance enhancement of a microgrid: A novel MPC approach," *Applied Energy*, vol. 333, 2023, doi: 10.1016/j.apenergy.2023.120639.

[10] A. K. Mishra, P. Mishra, and H. D. Mathur, "A deep learning assisted adaptive nonlinear deloading strategy for wind turbine generator integrated with an interconnected power system for enhanced load frequency control," *Electric Power Systems Research*, vol. 214, 2023, doi: 10.1016/j.epsr.2022.108960.

[11] H. A. Yousef, "Power System Load Frequency Control: Classical and Adaptive Fuzzy Approaches," *CRC Press*, 2017, doi: 10.1201/9781315166292.

[12] J. H. Li, "3d trajectory tracking of underactuated non-minimum phase underwater vehicles," *Automatica*, vol. 155, 2023, doi: 10.1016/j.automatica.2023.111149.

[13] M. Yadav, "An enhancement in series cascade control for non-minimum phase system," *Chemical Product and Process Modeling*, vol. 18, no. 1, 2023, doi: 10.1515/cppm-2021-0046.

[14] X. Lai, H. Huang, B. Zheng, D. Li, and Y. Zong, "Nonlinear modeling and stability analysis of asymmetric hydro-turbine governing system," *Applied Mathematical Modelling*, vol. 120, 2023, doi: 10.1016/j.apm.2023.03.012.

[15] B. Xu, J. Zhang, M. Egusquiza, D. Chen, F. Li, P. Behrens, and E. Egusquiza, "A review of dynamic models and stability analysis for a hydro-turbine governing system," *Renewable and Sustainable Energy Reviews* vol. 144, 2021, doi: 10.1016/j.rser.2021.110880.

[16] C. Wang, D. Wang, and J. Zhang, "Experimental study on isolated operation of hydro-turbine governing system of Lunzua hydropower station in Zambia," *Renewable Energy*, vol. 180, pp. 1237–1247, 2021, doi: 10.1016/j.renene.2021.09.014.

[17] P. Xu, W. Fu, Q. Lu, S. Zhang, R. Wang, and J. Meng, "Stability analysis of hydro-turbine governing system with sloping ceiling tailrace tunnel and upstream surge tank considering nonlinear hydro-turbine characteristics," *Renewable Energy*, vol. 210, pp. 556–574, 2023, doi: 10.1016/j.renene.2023.04.028.

[18] B. Sonker, D. Kumar, and P. Samuel, "Dual loop IMC structure for load frequency control issue of multi-area multi-sources power systems," *International Journal of Electrical Power and Energy Systems*, vol. 112, pp. 476–494, 2019, doi: 10.1016/j.ijepes.2019.04.042.

[19] T. Berger, "Tracking with prescribed performance for linear non-minimum phase systems," *Automatica*, vol. 115, 2020, doi: 10.1016/j.automatica.2020.108909

[20] Y. Li, J. Bi, W. Han, and W. Tan, "Tuning of $PID/PIDD^2$ controllers for integrating processes with robustness specification," *ISA Transactions*, vol. 140, pp. 224–236, 2023, doi: 10.1016/j.isatra.2023.05.015 .

[21] C. J. Munaro, M. R. Pimentel, R. B. D. Capaci, and L. Campestrini, "Data driven performance monitoring and retuning using PID controllers," *Computers and Chemical Engineering*, vol. 178, 2023, doi: 10.1016/j.compchemeng.2023.108360.

[22] P. Patil, S. S. Anchan, and C. S. Rao, "Improved PID controller design for an unstable second order plus time delay non-minimum phase systems," *Results in Control and Optimization*, vol. 7, 2022, doi: 10.1016/j.rico.2022.100117.

[23] T. Shuprajhaa, S. K. Sujit, and K. Srinivasan, "Reinforcement learning based adaptive PID controller design for control of linear/nonlinear unstable processes," *Applied Soft Computing*, vol. 128, 2022, doi: 10.1016/j.asoc.2022.109450.

[24] A. Rehan, I. Boiko, and Y. Zweiri, "Optimal non-parametric tuning of PID controllers based on classification of shapes of oscillations in modified relay feedback test," *Journal of the Franklin Institute*, vol. 358, pp. 1448–1474, 2021, doi: 10.1016/j.jfranklin.2020.12.007.

[25] Q. A. Mahmood and A. T. Nawaf, "Performance analysis of continuous stirred tank heater by using PID-cascade controller," *materialstoday: Proceedings*, vol. 42, pp. 2545–2552, 2021, doi: 10.1016/j.matpr.2020.12.577.

[26] J. Sun, G. Su, X. Chen, and W. Yang, "Switchable PID controller tuning based on golden section reduction rule," *IFAC-PapersOnLine*, vol. 53, no. 2, pp. 11068–11073, 2020, doi: 10.1016/j.ifacol.2020.12.244

[27] Y. Bouzid, H. Siguerdidjssane, and E. Zareb, "Improved IMC-filter design and IMC-PI equivalence: Application to quadrotor under gust of wind," *Proceedings of the Institution of Mechanical Engineers. Part I: Journal of Systems and Control Engineering*, vol. 234, no. 9, 2020, doi: 10.1177/09596518198941.

[28] I. Pisa, A. Morell, J. L. Vicario, and R. Vilanova, "LSTM-based IMC approach applied in Wastewater Treatment Plants: performance and stability analysis analysis," *IFAC-PapersOnLine,* vol. 53, no. 2, pp. 16569–16574, 2020, doi: 10.1016/j.ifacol.2020.12.782.

[29] P. Wang, Z. Chen, L. Liao, J. Wan, and S. Wu, "A multiple-model based internal model control method for power control of small pressurized water reactors," *Energy*, vol. 210, 2020, doi: 10.1016/j.energy.2020.118527

[30] K. B. Jemaa, P. Kotman, S. Reimann, and K. Graichen, "Tube-based internal model control of minimum-phase input-affine MIMO systems under input constraints," *IFAC-PapersOnLine*, vol. 53, no. 2, pp. 1677–1683, 2020, doi: 10.1016/j.ifacol.2020.12.2231.

[31] A. Mesbah, J. A. Paulson, and R. D. Braatz, "An internal model control design method for failure-tolerant control with multiple objectives," *Computers and Chemical Engineering*, vol. 140, 2020, doi: 10.1016/j.compchemeng.2020.106955.

[32] B. Zhang, W. Tan, and J. Li, "Tuning of smith predictor based generalized ADRC for time-delayed processes via IMC," *ISA Transactions*, vol. 99, pp. 159–166, 2020, doi: 10.1016/j.isatra.2019.11.002.

[33] T. Ikezaki and O. Kaneko, "Simultaneous update of controller and model by using virtual internal model tuning," *IFAC-PapersOnLine,* vol. 53, no. 2, pp. 4468–4473, 2020, doi: 10.1016/j.ifacol.2020.12.448.

[34] N. Li, H. Yang, W. Zhu, and C. Liu, "A novel grey decision-DE optimized internal model controller for vibration control of nonlinear uncertain aeroelastic blade system," *ISA Transactions*, vol. 107, pp. 27–39, 2020, doi: 10.1016/j.isatra.2020.07.036 .

[35] J. Xie, C. R. Koch, and S. Dubljevic, "Internal model controller design of linearized Ginzburg-landau equation," *IFAC-PapersOnLine,* vol. 53, no. 2, pp. 7728–7733, 2020, https://doi.org/10.1016/j.ifacol.2020.12.1523.

[36] T. Huang, G. Hu, Z. Meng, and D. Zeng, "IMC-based diesel oxidation catalyst outlet temperature control with extended state predictor observer," *Control Engineering Practice*, vol. 117, 2021, doi: 10.1016/j.conengprac.2021.104939.

[37] K. H. Park, T. W. Kim, Y. J. Kim, N. Lee, and Y. Seo, "Experimental investigation of model-based IMC control of severe slugging," *Journal of Petroleum Science and Engineering*, vol. 204, 2021, doi: 10.1016/j.petrol.2021.108732.

[38] E. Takahashi and O. Kaneko, "Data-driven internal model controller for mechanical systems with friction," *IFAC-PapersOnLine,* vol. 54, no. 14, pp. 233–238, 2021, doi: 10.1016/j.ifacol.2021.10.358.

[39] G. Vasu, M. S. Kumar, and M. R. Raju, "Internal model control design based on approximation of linear discrete dynamical systems," *Applied Mathematical Modelling*, vol. 97, pp. 683–700, 2021, doi: 10.1016/j.apm.2021.04.017.

[40] M. Yadav, H. G. Patel, and K. Shipra, "The combined effect of IMC controller and compensator for three-level dc-dc boost converter," *IFAC-PapersOnLine*, vol. 55, no. 1, pp. 454–459, 2022, doi: 10.1016/j.ifacol.2022.04.075.

[41] P. P. Arya, "A modified IMC design for second order plus time delayed processes," *IFAC-PapersOnLine,* vol. 55, no. 1, pp. 843–847, 2022, doi: 10.1016/j.ifacol.2022.04.138.

[42] S. Palomino, A. Gutarra, A. Quispe, E. J. Alegria and C. Diaz, "Control of a Water Tank Level Process Using IMC Controller," *2022 IEEE ANDESCON*, pp. 1-5, 2022, doi: 10.1109/ANDESCON56260.2022.9989679.

[43] N. Amuthan, M. B. M, P. Velrajkumar, N. Sivakumar, and T. Jarin, "IOT based adjustment mechanism for direct reference model adaptive IMC to support voltage sag in DFIG wind farm," *Measurement: Sensors*, vol. 27, 2023, doi: 10.1016/j.measen.2023.100809.

[44] S. Lim, Y. Yook, J. P. Heo, C. G. Im, K. H. Ryu, and S. W. Sung, "A new PID controller design using differential operator for the integrating process," *Computers and Chemical Engineering*, vol. 170, 2023, doi: 10.1016/j.compchemeng.2022.108105.

[45] P. Li and G. Zhu, "IMC-based PID control of servo motors with extended state observer," *Mechatronics*, vol. 62, 2019, doi: 10.1016/j.mechatronics.2019.102252.

[46] P. Li and G. Zhu, "Robust internal model control of servo motor based on sliding mode control approach," *ISA Transactions*, vol. 93, pp. 199–208, 2019, doi: 10.1016/j.isatra.2019.03.021.

[47] M. Kumar, D. Prasad, B. S. Giri, and R. S. Singh, "Temperature control of fermentation bioreactor for ethanol production using IMC-PID controller," *Biotechnology Reports*, vol. 22, 2019, doi: 10.1016/j.btre.2019.e00319.

[48] M. Irshad and A. Ali, "IMC based robust PI/PID controllers for time-delayed inverse response processes," *ISA Transactions*, vol. 134, pp. 278–289, 2023, doi: 10.1016/j.isatra.2022.09.001.

[49] R. Sanchis and I. P. Alos, "A new method for experimental tuning of PI controllers based on the step response," *ISA Transactions*, vol. 128, pp. 329–342, 2022, doi: 10.1016/j.isatra.2021.09.008.

[50] S. K. Chiluka, S. R. Ambati, S. H. Sonawane, M. M. Seepana, and U. B. B. Gara, "Robust IMC-PID controller design using VRFT: Theoretical and experimental investigation," *IFAC-PapersOnLine,* vol. 55, no. 1, pp. 241–246, 2022, doi: 10.1016/j.ifacol.2022.04.040.

[51] U. M. Nath, C. Dey, and R. K. Mudi, "Stabilized IMC-PI controller designing for IPDT processes based on gain and phage margin criteria," *IFAC-PapersOnLine,* vol. 53, no. 1, pp. 129–134, 2020, doi: 10.1016/j.ifacol.2020.06.022.

[52] W. Zeng, W. Zhu, T. Hui, L. Chen, J. Xie, and T. Yu, "An IMC-PID controller with particle swarm optimization algorithm for MSBR core power control," *Nuclear Engineering and Design*, vol. 360, 2020, doi: 10.1016/j.nucengdes.2020.110513.

[53] S. Y. Bhuran, and S. P. Jadhav, "Design and Analysis of IMC based Load Frequency Controller for NMP – Hydro Turbine Power System," *Turkish Journal of Computer and Mathematics Education*, vol. 12, no. 14, 2021, doi: 10.17762/turcomat.v12i14.12176.

[54] B. Doraswamy and K. L. Krishna, "Design and performance analysis of a novel vulture based FOPID controller for the nonlinear biological system," *Scientific African*, vol. 22, 2023, doi: 10.1016/j.sciaf.2023.e01892.

[55] Q. Han, L. Wang, L. Marconi, Z. Liu, and H. Su, "Adaptive control of non-linear systems with sinusoidal uncertainties via internal model principle," *IFAC-PapersOnLine*, vol. 56, no. 1, pp. 270–275, 2023, doi: 10.1016/j.ifacol.2023.02.046.

[56] Y. H. Lee and S. M. Su, "An all-pass based internal model principle controller for galvanometer mirror steering," *Control Engineering Practice*, vol. 141, 2023, doi: 10.1016/j.conengprac.2023.105696.

[57] A. Ranjan, U. Mehta, and S. Saxena, "A comprehensive review of modified internal model control (IMC) structures and their filters for unstable processes," *Annual Reviews in Control*, vol. 56, 2023, doi: 10.1016/j.arcontrol.2023.04.006.

[58] N. Zhu, X. T. Gao, and C. Q. Huang, "A data-driven approach for on-line auto-tuning of minimum variance PID controller," *ISA Transactions*, vol. 130, pp. 325–342, 2022, doi: 10.1016/j.isatra.2022.04.001.

[59] M. Venkatesh, S. Patra, and G. Ray, "Design of a set of stabilizing P and PI controllers for LTI TITO system with multiple time-delays," *IFAC-PapersOnLine*, vol. 55, no. 1, pp. 405–410, 2022, doi: 10.1016/j.ifacol.2022.04.067.

[60] S. A. Pavadaisami, M. T. A. Musthafa, and V. K. N. Jeganathan, "Particle swarm optimization based dual -mode fractional order control for automatic generation control of two area interconnected hybrid system," *International Journal of Intelligent Engineering and Systems*, vol. 15, no. 4, pp. 86–96, 2022, doi: 10.22266/ijies2022.0831.09.

[61] T. Berger and L. Lanza, "Output tracking for a non-minimum phase robotic manipulator," *IFAC-PapersOnLine,* vol. 54, no. 9, pp. 178–185, 2021, doi: 10.1016/j.ifacol.2021.06.074.

[62] P. Patil, S. S. Anchan, C. S. Rao, "Improved PID controller design for an unstable second order plus time delay non-minimum phase systems," *Results in Control and Optimization*, vol. 7, 2022, doi: 10.1016/j.rico.2022.100117.

[63] M. Patil, B. Bandyopadhyay, D. Khimani, and M Toe, "Robust output tracking for the non-minimum phase over-actuated systems," *Automatica*, vol. 131, 2021, doi: 10.1016/j.automatica.2021.109726.

[64] S. K. Chiluka, S. R. Ambati, M. M. Seepana, and U. B. B. Gara, "A novel robust Virtual Reference Feedback Tuning approach for minimum and non-minimum phase systems," *ISA Transactions*, vol. 115, pp. 163-191, 2021, doi: 10.1016/j.isatra.2021.01.018.

[65] S. Galeani, C. Possieri, and M. Sassano, "Output tracking for a class of non-minimum phase nonlinear systems: A two-point boundary value problem formulation with a hybrid regulator," *European Journal of Control*, vol. 58, pp. 43-52, 2021, doi: 10.1016/j.ejcon.2021.01.001.

[66] M. A. Z. Juárez, C. R. F. Ortiz, V. H. G. Cobián, B. M. L. Rebollar, I. G. Alarcón, and D. G. Pulido, "Parametric assessment of a Pelton turbine within a rainwater harvesting system for micro hydro-power generation in urban zones," *Energy for Sustainable Development*, vol. 73, pp. 101-115, 2023, doi: 10.1016/j.esd.2023.01.015.

[67] D. Liu, C. Li, and O. P. Malik, "Nonlinear modeling and multi-scale damping characteristics of hydro-turbine regulation systems under complex variable hydraulic and electrical network structures," *Applied Energy*, vol. 293, 2021, doi: 10.1016/j.apenergy.2021.116949.

[68] S. Rangi, S. Jain, and Y. Arya, "Utilization of energy storage devices with optimal controller for multi-area hydro-hydro power system under deregulated environment," *Sustainable Energy Technologies and Assessments*, vol. 52, 2022, doi: 10.1016/j.seta.2022.102191.

[69] D. Chen, C. Ding, X. Ma, P. Yuan, and D. Ba, "Nonlinear dynamical analysis of hydro-turbine governing system with a surge tank," *Applied Mathematical Modelling*, vol. 37, no. 14–15, pp. 7611–7623, 2013, doi: 10.1016/j.apm.2013.01.047.

[70] S. Huang, B. Zhou, S. Bu, C. Li, C. Zhang, H. Wang, and T. Wang, "Robust fixed-time sliding mode control for fractional-order nonlinear hydro-turbine governing system," *Renewable Energy*, vol. 139, pp. 447-458, 2019, doi: 10.1016/j.renene.2019.02.095.

[71] S. C. M, R. Honnasiddaiah, V. Hindasageri, and V. Madav, "Studies on application of vertical axis hydro turbine for sustainable power generation in irrigation channels with different bed slopes", *Renewable Energy*, vol. 163, pp. 845-857, 2021 doi: 10.1016/j.renene.2020.09.015.

[72] A. Ali, G. Biru, B. Banteyirga, "Fuzzy Logic-Based AGC and AVR for Four-Area Interconnected Hydro Power System," *Electric Power Systems Research*, vol. 224, 2023, doi: 10.1016/j.epsr.2023.109494.

[73] Q. Zhong, S. Hu, L. Yan, H. Zhou, J. Yang, K. Shi, and S. Zhong, "Adaptive event-triggered PID load frequency control for multi-area interconnected wind power systems under aperiodic DoS attacks," *Expert Systems with Applications*, vol. 241, 2024, doi: 10.1016/j.eswa.2023.122420.

[74] S. Tripathi, V. P. Singh, N. Kishor, and A. S. Pandey, "Load frequency control of power system considering electric Vehicles' aggregator with communication delay," *International Journal of Electrical Power & Energy Systems*, vol. 145, 2023, doi: 10.1016/j.ijepes.2022.108697.

[75] N. Sanchez, C. J. Dent, A. Wilson, "Statistical modelling of dependence between net demands and deficits in two area power systems," *Sustainable Energy, Grids and Networks*, vol. 36, 2023, doi: 10.1016/j.segan.2023.101151.

[76] B. Singh, and S. K. Bishnoi, "Bull-lion Optimization-based Proportional Integrated Derivative controller for regulating frequency in Two-Area Multi-Source power system," *Advances in Engineering Software*, vol. 181, 2023, doi: 10.1016/j.advengsoft.2023.103444.

[77] G. Cao, X. Zhang, P. Li, F. Li, Y. Liu, and Z. Wu, "Load frequency regulation of multi-area power systems with communication delay via cascaded improved ADRC," *Energy Reports*, vol. 9, pp. 983-991, 2023, doi: 10.1016/j.egyr.2023.04.379.

[78] A. Pepiciello, T. Pietropaoli, and A. Vaccaro, "Enabling technologies for resilient time synchronization of wide area power system monitoring,"

Encyclopedia of Electrical and Electronic Power Engineering, pp. 88-98, 2023, doi: 10.1016/B978-0-12-821204-2.00132-X.

[79] M. H. Fini, M. E. H. Golshan, J. R. Marti, and A. Ketabi, "Appropriate models for designing frequency control schemes in power systems," *Electric Power Systems Research*, vol. 228, 2024, doi: 10.1016/j.epsr.2023.110093.

[80] J. Koudelka, S. Macejko, T. Haba, B. Batora, and P. Toman, "Use of new means for frequency support of power system in emergency state," *Sustainable Energy, Grids and Networks*, vol. 37, 2024, doi: 10.1016/j.segan.2023.101239.